Check for updates

Journal of Biogeography

WILEY

Journal of Biogeography

RESEARCH ARTICLE OPEN ACCESS

Unveiling the Role of Spatial Functional Trait Variations on Grassland Primary Productivity at France Scale

Sara Chebbo[1] | Cyrille Violle[2] | Lucie Mahaut[2] | Jens Kattge[3] | Marc Peaucelle[4] | Philippe Choler[5] | Nicolas Viovy[1]

[1]LSCE/IPSL, CEA-CNRS-UVSQ, Université Paris-Saclay, Orme Des Merisiers, Gif-sur-Yvette, France | [2]CEFE, Université Montpellier, CNRS, EPHE, IRD, Montpellier, France | [3]Max Planck Institute for Biogeochemistry, Jena, Germany | [4]INRAE, Université de Bordeaux, Villenave-d'Ornon, France | [5]Université Grenoble Alpes, CNRS, LECA, Grenoble, France

Correspondence: Sara Chebbo (sara.chebbo@lsce.ipsl.fr)

Received: 24 July 2024 | **Revised:** 3 December 2024 | **Accepted:** 17 December 2024

Funding: This work was supported by the Commissariat à l'énergie atomique et aux énergies alternatives (CEA) and CLAND Convergence Institute.

Keywords: biodiversity | climate change | community weighted means | field data | functional biogeography | grassland primary productivity | land surface model | leaf economic spectrum | satellite observations | terrestrial biosphere model

ABSTRACT

Aim: Land surface models (LSMs) currently represent each plant functional type (PFT) as an average phenotype, characterised by a set of fixed parameters. This rigid and constant representation is a limit in understanding the dynamics of highly diverse ecosystems, such as permanent grasslands, and their response to global change.

Location: France.

Time Period: 2001–2019.

Major Taxa: Grassland plant species.

Methods: We incorporated spatially explicit trait variability at the France scale in the ORCHIDEE land surface model to assess how the net primary productivity (NPP) will spatially vary over the years. More precisely, we focused on three key functional traits that govern the NPP of grassland ecosystems: specific leaf area (SLA) and leaf nitrogen content (LNC), as measured traits, and leaf lifespan (LLS) as an estimated trait. Community-weighted means (CWM) were implemented in various combinations with prescribed and spatially varying traits. We compared the outcomes of each NPP simulation to remotely sensed proxies of productivity by using the MODIS satellite-driven NPP products.

Results: The sensitivity of NPP to traits depends on climate conditions, such as temperature and water limitation. Considering trait variability decreases the NPP in the most productive regions (plains) and increases the NPP in the less productive regions (mountains) compared to the case with constant trait values. This leads to a more homogenous NPP across France. Compared to the observed MODIS NPP and FLUXCOM GPP, the simulation using varying traits improves the spatial NPP and GPP variations in several regions and most climate conditions.

Main Conclusions: Based on the existing trait data, we revealed that incorporating the CWM of traits in an LSM such as ORCHIDEE can be effectively performed. Improving the modelling and predictions by considering the relationships between biodiversity, functional biogeography, and ecosystem functioning is essential in current and future ecological research.

1 | Introduction

Understanding vegetation dynamics and climate interactions at large spatial and temporal scales is a challenge in ecological research (Foley et al. 1996), especially in the current context of climate and land use changes. Land surface models (LSMs) and Dynamic global vegetation models (DGVMs) offer valuable tools to study ecosystem processes and their response to global environmental changes (Cramer et al. 2001; Sitch et al. 2003; Krinner et al. 2005; Bonan 2008). These models are

This is an open access article under the terms of the Creative Commons Attribution-NonCommercial-NoDerivs License, which permits use and distribution in any medium, provided the original work is properly cited, the use is non-commercial and no modifications or adaptations are made.

© 2025 The Author(s). *Journal of Biogeography* published by John Wiley & Sons Ltd.

developed and continuously updated based on scientific research, data collection, and model development (Fisher et al. 2018).

Trait-based ecology (TBE) (Lavorel and Garnier 2002; Violle et al. 2007) and the more recent emergence of functional biogeography (Violle et al. 2014; Garnier, Navas, and Grigulis 2015) have shed light on the importance of considering measurable characteristics of individuals to understand ecosystem functioning, particularly in the modelling field (Reichstein et al. 2014). Functional biogeography is defined as the analysis of the patterns, causes, and consequences of the geographic distribution of the trait diversity in forms and functions (Violle et al. 2014). Furthermore, the principle of scaling up from plant to community-level studies to evaluate trait-environment relationships has been pivotal to these disciplines (Shipley, Vile, and Garnier 2006; Enquist et al. 2015; Chacón-Labella et al. 2023) during the past years. Accordingly, functional traits have been used to predict ecosystem services and biodiversity responses across different environments (de bello et al. 2010; Lavorel and Grigulis 2012; Dias et al. 2013; Pan et al. 2021). Today, plant trait information can be found in multiple databases developed at local and global scales. Notably, the TRY plant trait database provides an unprecedented geographic coverage of trait measurements (Kattge et al. 2011, 2020). In recent years, efforts have been made in the land surface and dynamic global vegetation modelling field to include these data on plant functional traits and their variability and plasticity (Pavlick et al. 2013; Van Bodegom, Douma, and Verheijen 2014; Verheijen et al. 2015; Sakschewski et al. 2015).

LSMs generally represent the diversity of plant species by a set of plant functional types (PFTs) defined by a combination of constant parameters, some of them being directly related to plant functional traits (Sakschewski et al. 2015; Peaucelle et al. 2017). PFTs are classified by three main categories (crop, grass, and tree), leaf longevity (deciduous, evergreen), photosynthesis type (C3 or C4), and climate zone (boreal, temperate, and tropical). A well-acknowledged caveat of these models is the lack of consideration of trait variability and functional diversity across space and time (Van Bodegom et al. 2012; Díaz et al. 2007, 2016). By neglecting the full spectrum of trait variability and the effect of climate on this variability within species and communities, the uncertainties in the LSMs predictions tend to increase (Berzaghi et al. 2020). The ORCHIDEE (Organising Carbon and Hydrology In Dynamic Ecosystem Environment) model, a widely recognised LSM (Krinner et al. 2005), is not an exception, as its current representation of functional traits neglects the well-known variability of functional diversity in most biomes worldwide. Several studies have emphasised the importance of developing a new generation of trait-flexible vegetation models, but the lack of data was and still is the main barrier (Lavorel et al. 1997; Penone et al. 2014; Díaz et al. 2016).

Based on leaf data at the global scale, efforts have been made to describe a universal spectrum of leaf economic variation of key physiological, chemical, and structural properties by modulating trait relationships by climate (Wright et al. 2004). Community-weighted means (CWMs) is one of the methods used to calculate aggregated trait values within the community. For each trait, a mean value is computed by weighting the abundance of species within the community by the species trait values (Borgy et al. 2017b). This metric accounts for the effect of species abundances, which is essential to study ecosystem functioning, such as net primary productivity (NPP) (Garnier et al. 2004). Here, we have introduced new research to incorporate CWMs in a terrestrial biosphere model, marking an advancement in this field.

Building a bridge between functional biogeography and land surface modelling is a goal for both ecologists and modellers to forecast ecosystem functioning and services effectively. In this study, the main objective is to examine how LSM outcomes can be improved by incorporating CWMs of traits, using French permanent grasslands (FPGs) as a case study. Permanent grasslands are grasslands that have been used for at least 5 years to produce forage and that have not been ploughed or re-seeded during this period (Plantureux, Pottier, and Carrère 2012). Permanent grasslands provide major ecosystem functions and services due to the high biodiversity, the ability to adapt to diverse environmental conditions, and the unique functional traits found in grassland species and communities. Thus, the enhancement of understanding the impact of functional biogeography on grassland productivity across space is a current topic of interest in the ecological field. In ORCHIDEE, FPGs belong to a unique PFT (i.e., PFT 10), which represents the C3 herbaceous vegetation, including permanent grasslands. The objective of this paper is to integrate the functional biogeography of permanent grasslands into ORCHIDEE to simulate NPP for the 2001–2019 time period. We considered an explicit spatial distribution for three key traits of the leaf economic spectrum (LES) that govern NPP (Wright et al. 2004), and tested how individual traits alone or in combination influence NPP and community responses to environmental changes. We investigated the consequences of accounting for trait variability on NPP spatial variations and examined how closely model outcomes align with remotely sensed proxies of NPP using MODIS data.

2 | Data and Methods

2.1 | General Description of the ORCHIDEE Model

ORCHIDEE is a DGVM that includes two main modules: SECHIBA (mapping of hydrological exchange at the biosphere-atmosphere interface) and STOMATE (Saclay-Toulouse-Orsay Model for the Analysis of terrestrial ecosystems) (see—Krinner et al. 2005, Figure 2). The SECHIBA module focuses on the energy-water-CO2 exchanges between the biosphere and the atmosphere and the water budget in the soil (Ducoudré, Laval, and Perrier 1992). The STOMATE module represents various processes, such as carbon allocation, maintenance and growth respiration, soil carbon dynamics, litter decomposition, and phenology (Viovy and de Noblet 1997).

In this study, we used the 2.2 version (rev. 6756) (Krinner et al. 2005) of the ORCHIDEE model that classifies ecosystems into 13 different plant functional types (PFTs). We focused on PFT 10, representing grasslands inhabited by C3 herbaceous species and the effect of the trait variability on the NPP dynamics within this PFT.

2.2 | Vegetation and Plant Trait Data

As a vegetation map, we used the spatial distribution of FPGs (Borgy et al. 2017a), obtained by combining the European Corine land cover (CLC) and the Registre parcellaire Graphique database to map the grasslands at the France scale (Violle et al. 2015). The maps of community-weighted means (CWM) were gridded for traits of the leaf economic spectrum and were calculated by weighting the average value of species traits by the relative abundance of species found in the community. A total of 2930 species were included in the Divgrass database and used to derive the CWMs. A classification of four types of grassland—mesic, calcareous, mountainous, and ruderal—was defined thanks to a modularity analysis (Denelle, Violle, and Munoz 2020). The local species abundances were derived mainly from local vegetation relevés datasets, and the floristic data was completed by trait data using the TRY database, a global trait database initiative (Kattge et al. 2020), and other local databases (Borgy et al. 2017a). These CWM maps are called fixed CWM,

13652699, 0, Downloaded from https://onlinelibrary.wiley.com/doi/10.1111/jbi.15079 by MPI 322 Chemical Ecology, Wiley Online Library on [16/01/2025]. See the Terms and Conditions (https://onlinelibrary.wiley.com/terms-and-conditions) on Wiley Online Library for rules of use; OA articles are governed by the applicable Creative Commons License

not specific CWM (Lepš et al. 2011), because a single mean trait value is attributed to species found in each habitat. The within-species variability in traits is not considered in the calculation method of Borgy et al. (2017a).

We used the derived map extended to the whole FPGs based on the direct measurements issued from the relevés. As shown in (Violle et al. 2015) for leaf dry mass content (LDMC), it was possible to derive maps of traits across all the FPGs using a linear regression between CWM and growing season length dependent on temperature and soil water (GSL_{tw}) multiplied by nitrogen input. The same maps were derived for the specific leaf area (SLA, m^2/kg) and the leaf nitrogen content (LNC, mg/g) (Borgy et al. 2017a) using the LOESS (LOcally Estimated Scatterplot Smoothing) method (Gijbels and Prosdocimi 2010) instead of the linear regression to account for the nonlinearity of the relationships (Borgy, Personal communication). In the Borgy et al. (2017a, 2017b) approach, the community-level spatial trait variability at the France scale was mapped for only four traits: the specific leaf area (SLA), leaf nitrogen content (LNC), seed mass, and height for which a sufficient number of individual traits (NIV) per species is found. They reported that 17.4%, 14.2%, 55.2%, and 30.2% of species had available trait data for SLA, LNC, SM, and height, respectively. In the absence of sufficient direct measurements of Vcmax to derive a CWM map, Vcmax can be estimated from LNC. This estimation assumes a constant linear relationship between Vcmax and LNC as specified by Kattge et al. (2009). In this study, we used the CWM maps of two main traits based on empirical measurements, SLA and LNC. From LNC, we calculated the maximum rate of carboxylation (Vcmax, $\mu mol/m^2/s$), an existent trait in the model, by applying the following equation for C3 herbaceous from (Kattge et al. 2009):

$$\mathrm{Vcmax}(25) = 6.42 + 40.96 \times \mathrm{LNC_a}, \quad (1)$$

$$\mathrm{LNC_a} = \mathrm{LNC_m} \div \mathrm{SLA}$$

Vcmax(25) is the maximum photosynthesis rate per leaf area normalised to 25°C; LNC_a is the leaf nitrogen content per unit leaf area; LNC_m is the leaf nitrogen content per unit leaf mass; and SLA is the specific leaf area derived from the trait databases.

In addition to SLA and Vcmax, even if not mapped, a third important leaf trait is the leaf lifespan (LLS, days). In the absence of sufficient direct measurements of LLS to derive a CWM map, LLS can be estimated from SLA by assuming a constant linear relationship between LLS and SLA, as mentioned by Reich et al. (1999). As LLS is known to be coordinated with SLA and Vcmax (Reich et al. 1999), it is then important to also account for the spatial variability of this trait. Thus, we introduced a new parameterisation in ORCHIDEE to estimate LLS from SLA following the leaf economic spectrum (LES) after (Reich et al. 1999) instead of considering LLS as a fixed parameter like in the standard ORCHIDEE.

$$\mathrm{LLS} = 30.4 \times 10^{\frac{2.6215 - \log_{10}(SLA \times 5000)}{0.9}} \quad (2)$$

These traits are linked by trade-offs based on the leaf economic spectrum (Sakschewski et al. 2015) and are important to study the ability of plants to manage resources for photosynthesis and growth. In ORCHIDEE, the standard parameter values of SLA, Vcmax, and LLS for C3 grasslands are fixed to SLA = 13 m^2/kg, Vcmax = 50 $\mu mol/m^2/s$, and LLS = 80 days. These standard parameter values have been calibrated for global-scale applications.

We then used the spatial mean of SLA and Vcmax from CWM maps used to redefine standard parameters adapted to FPGs. Likewise, we performed a phenological parameters recalibration to ensure the accurate representation of the French phenological cycle, encompassing a correct start of the season and senescence. For this purpose, we used the 16 days MODIS NDVI at 0.05° resolution (http://doi.org/10.5067/MODIS/mod13c1.006) over FPGs to derive the beginning and end of the growing season (Moulin et al. 1997). The mean beginning and end of season over the period ranging from 2001 to 2019 were used to manually calibrate the main phenological parameters of ORCHIDEE (e.g., number of growing degree days, senescence temperature threshold).

2.3 | Climate, Vegetation, and Soil Input Data

We used variables from the SAFRAN atmospheric reanalysis (Vidal et al. 2010) as meteorological forcing to drive the ORCHIDEE model. The SAFRAN dataset was designed to provide a long-term gridded atmospheric dataset with a resolution of 8 km at the France scale on an hourly time step. The computed variables used are rainfall, snowfall, mean air temperature, climatology of surface pressure, specific humidity, wind speed, and solar and infrared radiation. We selected the meteorological data for the period extending from 1960 to 2019. We also used the annual CO_2 atmospheric concentration as a forcing variable available for the 1860–2020 period. The source of CO_2 data is attributed to the CO_2 forcing provided within the context of the TRENDY intercomparison project (Friedlingstein et al. 2022). In addition, we used the vegetation map of the FPGs, CWM SLA, and CWM Vcmax maps as forcing parameters (Violle et al. 2015; Borgy et al. 2017a). The original 5 km maps were interpolated to the 8 km grid of the SAFRAN meteorological forcing.

2.4 | Available Data for Simulation Comparison

At the France scale, the available NPP and GPP datasets are relatively scarce. On one hand, there are in situ flux measurements available from the ICOS network (Sabbatini et al. 2018). This data is more reliable but limited to a small number of FPG sites. On the other hand, NPP and GPP spatially explicit estimations are available at the French scale. The existing datasets are mainly derived from satellite observations or extrapolations based on site-specific measurements. Among these, the MODIS remote-sensed products estimate NPP (Running et al. 1999; Neumann et al. 2016), while the FLUXCOM products estimate GPP based on flux measurements (Jung et al. 2020).

For the comparison with in situ data, we studied three grassland sites of the Integrated Carbon Observation System (ICOS) network stations in France located in different geographical regions: Lusignan (plain grassland), Col du Lautaret (Alpine grassland, high elevation), and Laqueuille (Montane grassland, moderate elevation). These are the only three sites available for

13652699, 0, Downloaded from https://onlinelibrary.wiley.com/doi/10.1111/jbi.15079 by MPI 322 Chemical Ecology, Wiley Online Library on [16/01/2025]. See the Terms and Conditions (https://onlinelibrary.wiley.com/terms-and-conditions) on Wiley Online Library for rules of use; OA articles are governed by the applicable Creative Commons License

French grasslands that cover plains, mid-elevation, and high-elevation mountains. For these sites, net CO2 fluxes are estimated by eddy-correlation, and the GPP and total ecosystem respiration (Reco) are estimated from the net flux using the fact that GPP is null during the night data (Sabbatini et al. 2018). The first step is to simulate the GPP in each site by ORCHIDEE in 2023. The forcing variables are the meteorological data of each site (as detailed in Section 2.3) and the CO_2 concentration. The second step is to process a comparative analysis with the observed flux of GPP in 2023 in each site using daytime.

We conducted a comparative analysis between the simulated mean net primary productivity (NPP) values by the ORCHIDEE model in each of the five experiment cases (see—Table 1) and the satellite observations to assess the performance of the model. We compared the simulated mean NPP over the 2001–2019 period to the estimated NPP from the moderate resolution imaging spectroradiometer (MODIS) NPP product available for the same period (MOD17A3HGF) (Running et al. 1999). The MODIS NPP is first based on the GPP. This GPP uses a maximum light use efficiency model calibrated for each vegetation type and modulated by temperature and vapour pressure deficit. Then, NPP is estimated by subtracting the maintenance respiration from GPP. This maintenance respiration is estimated from a guess of plant biomass. This biomass is calculated from an empirical relationship between biomass and maximum leaf area index. Satellite products that estimate NPP, such as MODIS, are based on modelling because NPP cannot be directly mapped. This highlights the challenges and potential inaccuracies associated with using satellite-based products for NPP estimation.

First, we used the FPGs map at a 1×1 km scale to select only FPGs pixels from the global NPP MODIS dataset. Then, we reprojected it to the 8×8 km SAFRAN atmospheric reanalysis map (Vidal et al. 2010). We used a second available NPP MODIS product developed in Europe for the 2000–2012 time period (Neumann et al. 2016) to assess the uncertainty related to the remote sensed estimation of NPP. We also performed Kruskal–Wallis and post hoc Conover-Iman tests to evaluate potential simulated-estimated differences.

Then, we compared the simulated gross primary production (GPP) by the ORCHIDEE biosphere model at the France scale to the FLUXCOM GPP flux product. The FLUXCOM initiative aims to upscale the local eddy covariance (EC) flux tower measurements to global scale estimates of GPP based on machine learning methods (Jung et al. 2020). The EC is a technique to estimate the CO_2 and energy exchanges between Earth's surface and the atmosphere. The time period is 2001–2015 in this comparison.

2.5 | Simulation Experiments

We performed four distinct sets of simulations using the ORCHIDEE model. In the first set, we utilised the originally prescribed SLA and Vcmax for C3 temperate grasslands (namely fixstand). In the second set, we replaced the standard values with the mean CWM SLA and CWM Vcmax calculated from the CWM trait maps (namely, fixrecalc and fixrecalcllvar). For the third set, we integrated spatial SLA and Vcmax variability by including CWM SLA and CWM Vcmax maps in the model (namely, varllfix and varllvar). In opposition to SLA and Vcmax (thru LNC), LLS is not mapped but estimated by the model. For this reason, for the simulations based on variable traits, we consider two sets of simulations: one with a fixed LLS as in the standard version of ORCHIDEE and another with an estimated LLS from SLA. To study the impact of the leaf lifespan (LLS), which is estimated by the model, we conducted two sub-simulations within the second and third sets: one with a standard constant value for LLS, and the other with a varying LLS based on the SLA.

TABLE 1 | Comprehensive overview of the set of simulation types executed using the ORCHIDEE model for the 1960–2019 time period. The standard SLA and Vcmax values are, respectively, 13 m^2/kg and 50 μmol/m^2/s. The recalculated SLA and Vcmax values are, respectively, 21 m^2/kg and 56.4 μmol/m^2/s. When SLA and Vcmax values are variable, CWM SLA and CWM Vcmax are considered. In (a) and (b), the standard LLS is 80 days. In (c) and (d), the recalculated LLS is 64 days. In (e), LLS is variable and estimated from the CWM SLA.

	SLA and Vcmax values				LLS value	
Name of simulation	**Standard**	**Recalculated**	**Constant**	**Variable**	**Constant**	**Variable**
a. Fixstand	✓		✓		✓ (80 days)	
b. Fixrecalc		✓	✓		✓ (80 days)	
c. Fixrecalcllvar		✓	✓		✓ (64 days)	
d. Varllfix				✓	✓ (64 days)	
e. Varllvar				✓		✓

Name of simulation	**Simulation description**
a. Fixstand	Fixed trait values in the standard ORCHIDEE version
b. Fixrecalc	Fixed recalculated mean trait values from data with a standard LLS value
c. Fixrecalcllvar	Fixed recalculated mean trait values from data with a recalculated mean LLS
d. Varllfix	Variable trait values with a standard LLS fixed
e. Varllvar	Variable trait values with a variable LLS

13652699, 0, Downloaded from https://onlinelibrary.wiley.com/doi/10.1111/jbi.15079 by MPI 322 Chemical Ecology, Wiley Online Library on [16/01/2025]. See the Terms and Conditions (https://onlinelibrary.wiley.com/terms-and-conditions) on Wiley Online Library for rules of use; OA articles are governed by the applicable Creative Commons License

For all types of simulations on ORCHIDEE, we used a model spin-up for 20 years, using the first 10 years of climate in a loop, which is a sufficient duration to reach an equilibrium state for NPP and biomass pools in FPGs (Messina et al. 2016). Then, we conducted six consecutive series of simulations for 10 years each with actual climate ranging from 1960 to 2019. In this study, we selected the simulated NPP for the 2001–2019 time period considered as the common years for comparing the simulated NPP to the estimated MODIS global NPP.

Finally, a fourth set of simulations was performed to make a sensitivity analysis of NPP to SLA and Vcmax considering the observed range of values over France. The NPP sensitivity analysis was conducted by evaluating the difference between the simulated NPP with maximum SLA (respectively, Vcmax) and the NPP with minimum SLA (respectively, Vcmax) normalised by the mean NPP (see Table S1). We defined the SLA and Vcmax minimum and maximum values, respectively, as the average values of the 2nd and 98th percentiles of each trait map data. To evaluate NPP sensitivity to each of the two traits (i.e., SLA and Vcmax), we first fixed the other trait to its mean value. This simulation will be called hereafter "decoupled" (Table S1a). But, as SLA and Vcmax are correlated, we did a second set of simulations when the associated trait (i.e., Vcmax when considering SLA, SLA when considering Vcmax) was calculated by averaging the values of the associated trait for pixels with values close to the minimum and maximum. This simulation will be called hereafter "coupled" (Table S1a). Thus, we performed two sets of simulations: one with the SLA/Vcmax extreme value associated with the Vcmax/SLA mean value calculated from data and a second by coupling both SLA/Vcmax extreme values (see-Table S1).

For comparison with in situ data, we performed two simulations (namely fixrecalcllvar and varllvar) in each of the three French sites (i.e., Lusignan, Col du Lautaret and Laqueuille). The prescribed SLA/Vcmax and simulated LLS values for the three on-site simulations are presented in Table S2. To compare the simulations with each other and with the satellite observations, we did not directly look at the NPP but at the deviation of NPP for a given pixel to the spatial mean NPP for a given year, named Δ. Δ is calculated for each simulation by subtracting the simulated NPP from the average NPP of each of the following simulation types (i.e., fixrecalc, fixrecalcllvar, varllfix, and varllvar). On the other hand, Δ for the MODIS estimated NPP is calculated by subtracting the NPP values from the average of MODIS NPP. $\varepsilon_{sim} = \text{abs}(\Delta\text{sim} — \Delta\text{modis})$ is the absolute error between a simulated and estimated Δ. The error difference between two simulations $\delta\varepsilon = (\varepsilon_{sim1} - \varepsilon_{sim2})$ gives the increase or decrease of error in one simulation compared to the other one. Then a negative value of $\delta\varepsilon$ indicates a better agreement of NPP of sim1 than NPP of sim2 with MODIS NPP, while a positive value indicates the opposite case. The same methodology in Δ and $\delta\varepsilon$ is applied to compare the simulated GPP to the FLUXCOM GPP for the 2001–2015 time period.

Finally, we evaluated the NPP-climate relationships considering two climate variables: the mean annual temperature (MAT) and the growing season length defined from temperature and precipitation (GSL_{tw}) as defined in (Borgy et al. 2017a).

3 | Results

3.1 | Trait Mean Values and Maps

Figure 1 shows the spatial distribution of the absolute values of CWM of SLA, Vcmax, and LLS, respectively. The spatial distribution of the difference between CWMs and the default ORCHIDEE values, respectively, for SLA, Vcmax, and LLS estimated from the CWM SLA (Equation 2). is shown in Figure S5. The mean trait values of SLA and Vcmax recalculated from data at the France scale are 21.5 ± 0.028 (SE) m^2/kg. and 56.4 ± 0.05 (SE) μmol/m^2/s, respectively. The observed range of SLA is 16 m^2/kg to 24 m^2/kg and for Vcmax, it is 53 μmol/m^2/s to 66 μmol/m^2/s, which corresponds to a range of LNC of 18 g/kg to 34 g/kg. Kattge et al. 2011 report an observed range of SLA (at the species level) for C3 grasses of 6 m^2/kg to 55 m^2/kg and an LNC range from 10 g/kg to 48 g/kg. Then, the observed range of SLA and LNC is close to the lower values of the observed range in C3 grasslands based on the TRY database. The mean LLS value simulated by the model is 64 days. The recalculated mean SLA is there almost twice the original prescribed value (13 m^2/kg). The Vcmax is slightly higher than the standard value (50 μmol/m^2/s), and LLS is shorter than the standard value (80 days).

We mainly observe two clusters (Figure 1). The first one represents almost 80% of FPGs, corresponding to moderate and low-elevation grasslands. These grasslands have a higher SLA than the mean but in a narrow range between the mean (21.5 m^2/kg) and the maximum (23.4 m^2/kg) value. The remaining 20%, which are mainly located in high-elevation and some mid-elevation grasslands, have a largely lower SLA than the mean between 15 and 17 m^2/kg. This large difference in the size of these two clusters makes the mean SLA and Vcmax values very asymmetric compared to the range of values and then close to the upper bound of the SLA range (respectively lower bound for Vcmax).

Regions with lower SLA values have the highest Vcmax and LLS values (Figure 1). Then symmetrically to higher mean SLA, the mean Vcmax and the mean LLS are close to the minimum boundary of the Vcmax and the LLS range values.

3.2 | Sensitivity of NPP to Trait-Based Model Parameter Variation in Response to Climate

Figure 2 shows the sensitivity, for each pixel, of simulated NPP to the trait range in response to MAT and GSL, each trait coupled by the other one. Results for the decoupled mode are shown in Figure S7. The sensitivity to SLA and Vcmax is always positive in the decoupled cases (Figure S7) but becomes negative for SLA in the coupled mode (Figure 2) (i.e., higher SLA induces lower NPP because of the associated decrease of Vcmax). Likewise, the range of sensitivity variation (especially for Vcmax) is lower in coupled mode. The sensitivity of NPP to Vcmax is higher compared to SLA (Figures 2 and S7). The sensitivity of NPP to SLA increases with increasing MAT or GSL, but, on the contrary, it decreases for Vcmax. The linear regression slope of NPP sensitivity response to SLA and Vcmax is lower for GSL than for MAT

13652699, 0, Downloaded from https://onlinelibrary.wiley.com/doi/10.1111/jbi.15079 by MPI 322 Chemical Ecology, Wiley Online Library on [16/01/2025]. See the Terms and Conditions (https://onlinelibrary.wiley.com/terms-and-conditions) on Wiley Online Library for rules of use; OA articles are governed by the applicable Creative Commons License

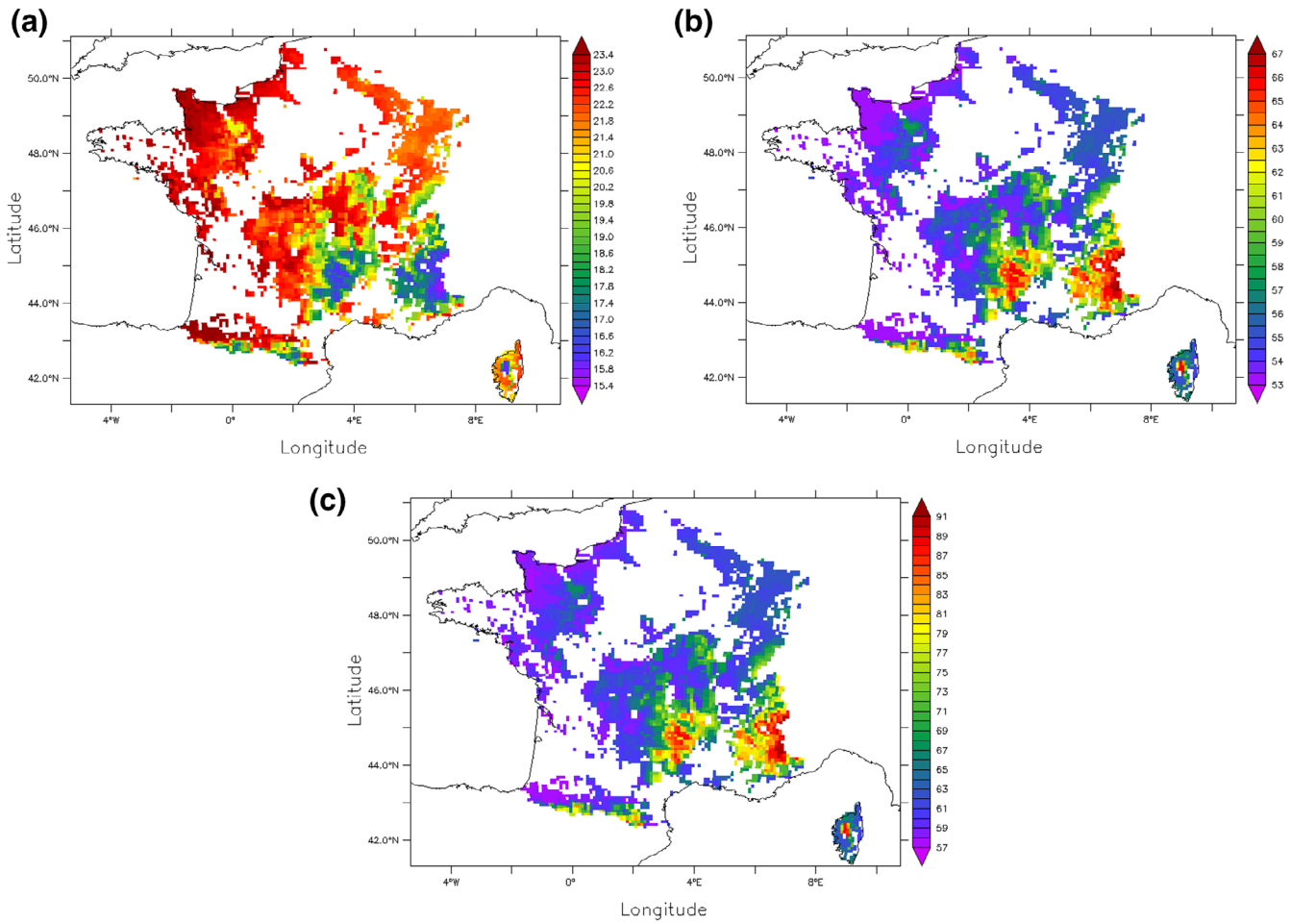

FIGURE 1 | Community weighted mean (CWM) maps of (a) the specific leaf area (SLA) in m^2/kg, (b) the maximum rate of carboxylation (Vcmax) in $\mu mol/m^2/s$, and (c) the estimated leaf life-span (LLS) in days. ORCHIDEE default values of SLA, Vcmax and LLS are respectively: 13 m^2/kg, 50 $\mu mol/m^2/s$ and 80 days.

in coupled and decoupled cases (e.g., slope = 0.0001 vs. 0.004 for sensitivity to SLA in coupled mode). For SLA, the positive relationship between sensitivity and MAT or GSL is only true for temperatures above 280 K (approximately 8.8°C) or GSL greater than 220 (Figures 2a,c and S7a,c). In particular, for MAT there is a bell-shaped response around 277 K (approximately 3.8°C; Figures 2 and S7a).

3.3 | Evaluation Against MODIS NPP and FLUXCOM GPP Products

The median NPP is higher when the mean SLA and Vcmax values calculated from CWM trait maps are prescribed or when using the variable trait distribution compared to the case with default trait values regardless of the value of LLS (80 or 64 days) (Figure 3I). The median of MODIS GLOBAL ($M = 768.35$) is almost at the mean between the median NPP in the fixstand case ($M = 695.73$) and the median NPP of the other four simulations ($M = 881.77$, $M = 866.56$, $M = 872.22$, $M = 866.93$). However, the median NPP in the fixstand case is very close to the MODIS EURO median ($M = 672.97$) and is the only simulation in the range of the observed MODIS NPP. However, it should be noticed that the difference between the median of the two MODIS products (medians difference = 95.38) is very similar to the difference observed between the median of each simulation (i.e., fixrecalc, varllfix, fixrecalcllvar, varllvar) and the median of MODIS GLOBAL mentioned above (Figure 3I). This was also observed when Cluster 1 of 80% of pixels mainly located in plains, and Cluster 2 of 20% of pixels mainly located in the mountains, were studied separately but with lower range values in Cluster 1 (Figure 3II,III). The Kruskal–Wallis test reveals a significant difference between the NPP median values of the five experiment cases and the two NPP MODIS products (Figure 3I,II,III). The post hoc Conover-Iman test shows a significant difference between the medians of all pairs of experiments and the two MODIS products (p_value < 0.05), except for the 'Fixstand-Modis global' and 'varllfix-varllvar' cases (Figure 3I). In both clusters, the Conover-Iman test shows a significant difference between the medians of pair groups (Figure 3II,III).

'fixrecalc' and 'fixrecalcllvar' show the highest correlation ($R^2 = 0.51$; Table 2), but, on the contrary, 'varllfix' and 'varllvar' show a lower RMSE (62 and 64 $gC/m^2/year$), indicating that the use of varying traits gives a better accuracy in the simulated NPP compared to the estimated MODIS GLOBAL NPP.

The different simulations show relatively similar NPP range values over France ($300 < NPP < 1155\ gC/m^2/year$) (Figure S1b,c), but

13652699, 0, Downloaded from https://onlinelibrary.wiley.com/doi/10.1111/jbi.15079 by MPI 322 Chemical Ecology, Wiley Online Library on [16/01/2025]. See the Terms and Conditions (https://onlinelibrary.wiley.com/terms-and-conditions) on Wiley Online Library for rules of use; OA articles are governed by the applicable Creative Commons License

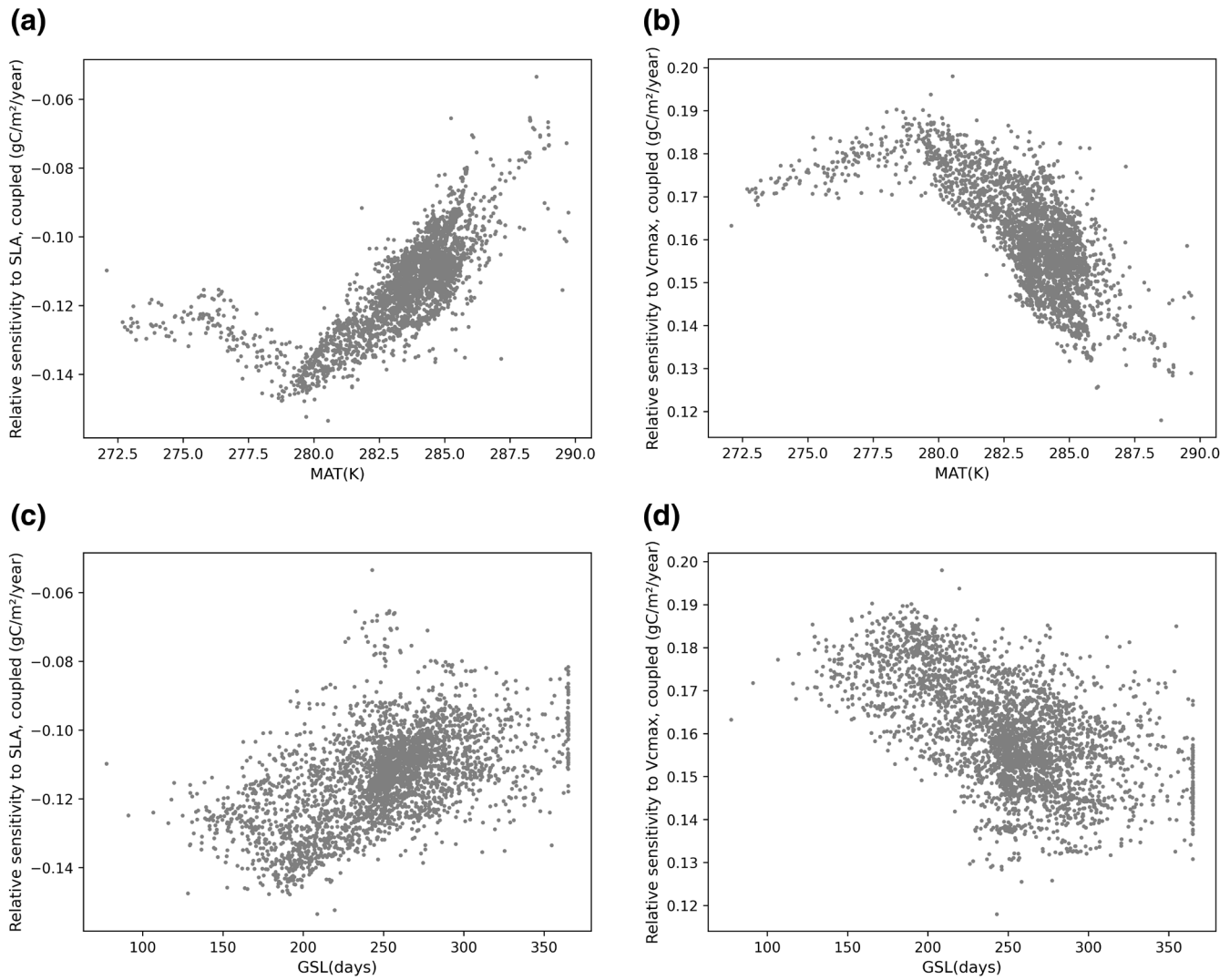

FIGURE 2 | Scatterplots of NPP sensitivity to SLA and Vcmax versus MAT and GSL (a) SLA vs MAT coupled (b) Vcmax vs MAT coupled (c) SLA vs GSL coupled (d) Vcmax vs GSL coupled. The time period is 2001–2019.

'fixstand' is systematically lower ($218 < NPP < 827$ gC/m^2/year) except for high-elevation regions (Figure S1a, zone a). The global range of annual NPP simulated by ORCHIDEE in all temperate C3 grasslands (i.e., PFT 10) in fixed stand case ranges from 150 gC/m^2 to 1100 gC/m^2. The simulations at the France level then cover a large range of simulated NPP across all temperate grasslands. For MODIS NPP, the distribution is more complex. In particular, the southwest of Massif Central shows a higher NPP ($800 < NPP < 900$ gc/m^2/year) than the rest of the region ($650 < NPP < 800$ gc/m^2/year) (Figure S1d, zone b), whereas simulated NPP is close as in the different simulations in this region (the majority of NPP ranging between 850 and 950 gC/m^2/year). Similar patterns are observed in Cotentin ($850 < NPP < 1000$ gC/m^2/year) (Figure S1b; zone a, S1c and S1d) except for the 'fixstand' case where NPP is lower than 800 gC/m^2/year. MODIS gives a lower NPP for the other surrounding regions (i.e., mountain, Mediterranean and some plain zones) (Figure S1d, zones d) ($250 < NPP < 800$ gC/m^2/year), compared to the simulated NPP when fixed or variable traits from data are used ($400 < NPP < 1000$ gC/m^2/year) (see Figure S1b–d). There is also a large difference in the south of the Alps (Figure S1c, zone e), where simulated NPP is close to the mean NPP (around 850 gC/m^2/year) over FPGs, whereas it is lower in the MODIS estimated NPP (mean NPP = 620 gC/m^2/year).

The simulations with variable traits (i.e., varllfix) compared to fixed traits (i.e., fixrecalc) show, on average a decrease of 25 gC/m^2/year in the plains and west of the Massif Central and an increase of 22 gC/m^2/year in the high and mid-elevation mountains (Figure S3a). The contrast between plains and mountains is increased when comparing the 'varllvar' and 'fixrecalcllvar' cases, showing a decrease of 21 gC/m^2/year in plains and west of the Massif Central (Figure 4, zones a and b respectively), which also correspond to high SLA/low Vcmax (Figure S5a,b) and an increase of 38 gC/m^2/year in high-elevation and some mid-elevation mountains (Figure 4, zones c and d respectively), where low SLA and high Vcmax are seen (Figures 4 and S5a,b). The same pattern is seen when comparing 'varllvar' to 'varllfix' case (Figure S3d), indicating that considering the variable LLS enhances the difference between spatially variable traits and fixed traits simulations. The large asymmetry in trait distribution (i.e., SLA mean close to the highest values and Vcmax means close to the lowest values) (Figure S5a,b), also explains

13652699, 0, Downloaded from https://onlinelibrary.wiley.com/doi/10.1111/jbi.15079 by MPI 322 Chemical Ecology, Wiley Online Library on [16/01/2025]. See the Terms and Conditions (https://onlinelibrary.wiley.com/terms-and-conditions) on Wiley Online Library for rules of use; OA articles are governed by the applicable Creative Commons License

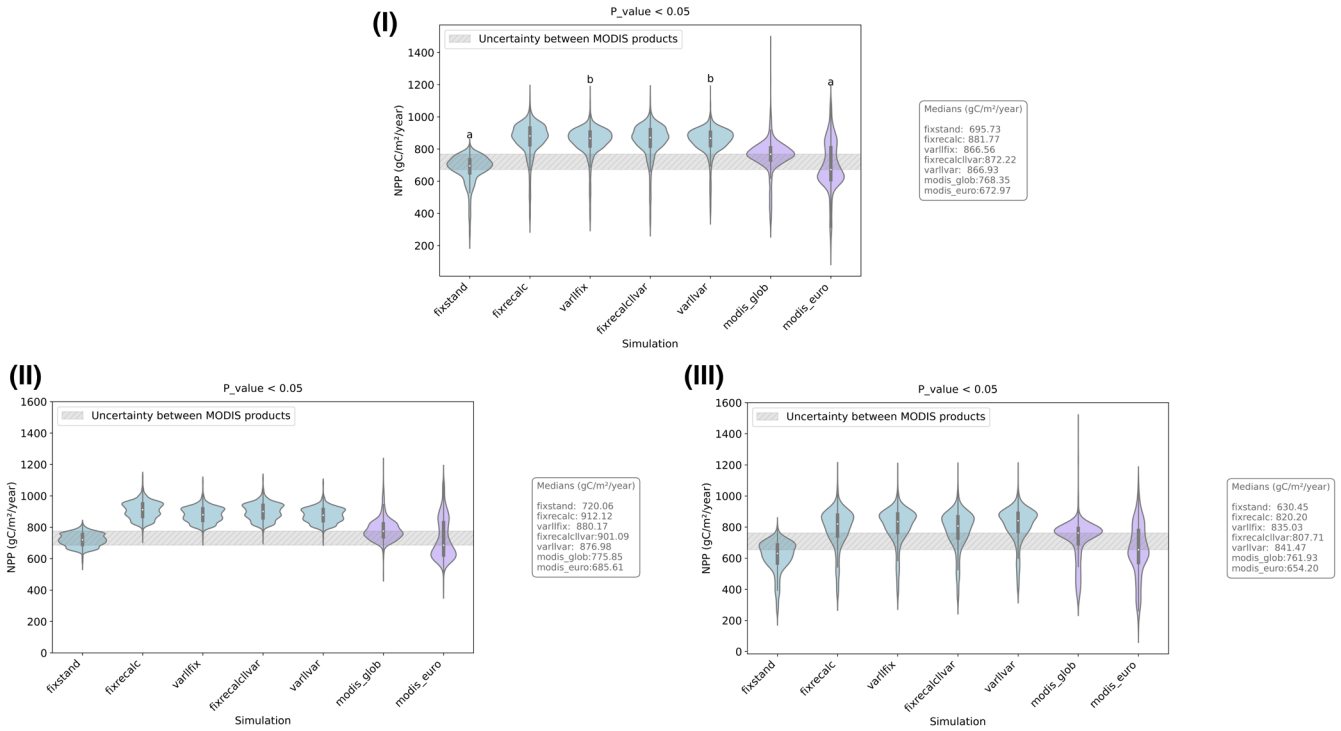

FIGURE 3 | Distribution of the simulated net primary productivity (NPP), estimated MODIS GLOBAL NPP for the 2001–2019 time period, estimated MODIS EURO for the 2000–2012 time period, and FLUXCOM GPP for the 2001–2015 time period. (I) All grasslands are combined, (II) Cluster 1 (80% of FPGs), (III) Cluster 2 (20% of FPGs). Kruskal–Wallis *p*_value is lower than 0.05 (significant difference) in (I), (II) and (III). In (I), the Conover-Iman *p*_value for each pair of experiment cases is lower than 0.05, except for the 'fixstand-modis euro' (a,a) and 'varllfix-varllvar' (b,b) cases, where the *p*_value is higher than 0.05 (not a statistically significant difference). In (II) and (II), no significant difference between all pairs of groups.

that a majority of pixels have a lower NPP than when using the mean trait but with a moderate decrease, whereas there are fewer pixels where NPP is higher but with a large increase.

Looking at the response of simulated and MODIS NPP to MAT shows a high positive correlation for MAT less than 280 K (Figure 5a). Above 280 K, there is no more increase of NPP with increasing MODIS NPP, whereas NPP continues to increase in both fixrecalcllvar and varllvar simulations. However, over 280 K, the slope of the response of NPP to MAT is lower for 'varllvar' (28 gC/m^2/year per K) than 'fixrecalcllvar' (40.3 gC/m^2/year per K). This implies a lower sensitivity of NPP to MAT changes in the 'varllvar' case, as supported by the Pearson correlation coefficient $R = 0.78$ for 'varllvar' and $R = 0.88$ for 'fixrecalcllvar' (Figure 5a). Varllvar is then better in agreement with MODIS than fixrecalcllvar. The response of NPP to GSL, for both simulation and MODIS, shows a rapid increase in NPP with increasing GSL but only for GSL lower than 200 days. However, for GSL higher than 200 days, the increase of NPP with increasing GSL is limited with a large dispersion (Figure 5b).

As described in Section 2.5, we defined the parameter $\delta\varepsilon$ to measure the increase or decrease of the discrepancy between variable traits or fixed traits simulations compared to MODIS NPP. Negative values indicate an improvement of the simulated NPP compared to MODIS NPP, while positive values indicate the opposite case.

Compared to MODIS NPP and FLUXCOM GPP, $\delta\varepsilon$ of NPP and GPP is improved in both variable trait simulations compared to fixed trait simulations in most of the low-elevation regions (excluding the Cotentin (Figure 6a, zone a, and Figure 6b)) and high-elevation regions (except the south of the alps; Figure 6a, zone b and c, and Figure 6b). By contrast, $\delta\varepsilon$, is positive in the Mediterranean region (Figure 6a, zone c, and Figure 6b), where MODIS NPP gives a different pattern than simulations as discussed previously (i.e., southwest of the Massif Central and the Cotentin for instance) (Figure 6, Zones d & a respectively, & Figure S4).

More particularly, FLUXCOM shows more contrasted results with a stronger improvement and a more pronounced degradation in certain regions (Figure 6b). Despite these variations, FLUXCOM reveals a very high spatial coherence in areas where either improvements or degradations are observed compared to MODIS (e.g., a,b,c, and d zones) (Figure 6a,b).

We then looked at the response of $\delta\varepsilon$ (varllvar vs. fixrecalcllvar) to the two MAT and GSL climate variables. Since there are both positive and negative $\delta\varepsilon$ for all climate conditions, we calculated the mean $\delta\varepsilon$ for each value of MAT of GSL to see if, on average, $\delta\varepsilon$ is positive or negative, considered as the mean error between varllvar and fixrecalcllvar cases (Figure 7a,b). We can see that, for GSL lower than 345 days and MAT less than 287 K, $\delta\varepsilon$ is negative, indicating that varllvar is more in agreement with MODIS than fixrecalcllvar (Figure 7a,b). The variability for $\delta\varepsilon$ in response to MAT, as estimated from permutated data, is high, reflecting both the low number of samples and also the fact that there are contrasting results for these regions, with both negative and positive values. On the contrary, for GSL > 345 days and MAT > 287 K, $\delta\varepsilon$ is positive,

13652699, 0, Downloaded from https://onlinelibrary.wiley.com/doi/10.1111/jbi.15079 by MPI 322 Chemical Ecology, Wiley Online Library on [16/01/2025]. See the Terms and Conditions (https://onlinelibrary.wiley.com/terms-and-conditions) on Wiley Online Library for rules of use; OA articles are governed by the applicable Creative Commons License

TABLE 2 | Standardised major axis (SMA) analysis of the simulated NPP in each of the 5 cases of the experiment (*Y* axis) in function of the estimated NPP by MODIS at global scale (*X* axis). R^2: Squared correlation coefficient of the SMA, int: Intercept, CI: Confidence interval. Slope and intercept test *p*_value is lower than 0.05 (heterogeneous slopes) between each simulation and MODIS NPP. Kruskal–Wallis *p*_value is lower than 0.05 in all cases. The Conover_iman post hoc test *p*_value is lower than 0.05 in the 1–2, 1–3 and 2–3 pairs of groups.

Simulated NPP (Y)	R^2	Slope (Slope low CI–Slope high CI)	Intercept (int low CI–int high CI)	RMSE
1. Fixstand	0.46	0.86 (0.84–0.88)	20.39 (3.67–37.12)	65
2. Fixrecalc	0.51	1.03 (1–1.05)	80.92 (61.95–99.88)	73.7
3. Fixrecalcllvar	0.51	1.03 (1.01–1.06)	67.16 (48.12–86.2)	74
4. Varllfix	0.5	0.88 (0.86–0.91)	175.74 (159.28–192.21)	64
5. Varllvar	0.48	0.84 (0.82–0.86)	211.73 (195.8–227.66)	62

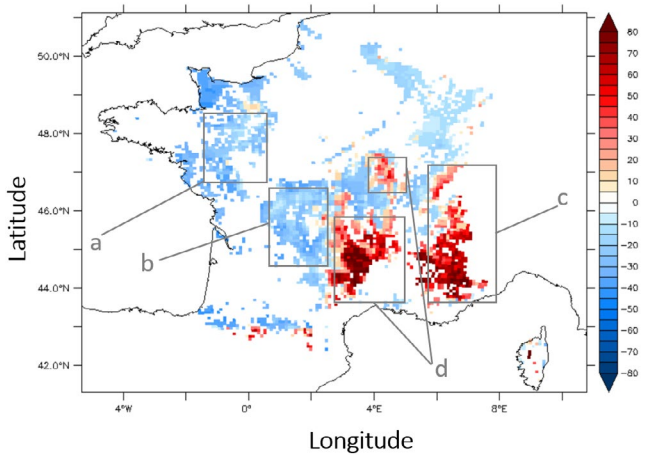

FIGURE 4 | Net primary productivity (NPP) difference between pairs of simulations (varllvar vs. fixrecalcllvar) for the 2001–2019 time period. Zones a,b,c, and d represent the areas cited in Section 3.3.

indicating that variable traits give results less in agreement with MODIS (Figure 7a,b). Results for variable trait cases are largely improved for low values of GSL/MAT, whereas they are only slightly less good for higher values.

3.4 | On-Site GPP Evaluation Against ICOS Flux Tower Data

We also compared the varllvar and fixrecalcllvar GPP simulations with in situ measurements of carbon fluxes from the flux tower of the ICOS network. From the measured carbon net flux, a flux of GPP is estimated and compared to the simulated flux (simulations performed using the in situ half-hourly meteorological parameters measured at the sites). Figure 8 shows the difference between simulated and observed GPP fluxes with a smoothing timestep of 10 days. The simulated GPP in the varllvar and fixrecalcllvar cases at Lusignan and Laqueuille is lower than the observed GPP (GPP DT) in 2023 during the growing season (Figure 8a,c). At Col du Lautaret, this is only true for the period from January through the end of June 2023, as the simulated GPP became higher than the observed GPP after July 2023 in both simulations (Figure 8b).

The differences between simulated GPP in the varllvar case and the fixrecalcllvar case (which uses the standard constant traits for France) are very similar at Lusignan (Figure 8a). This is not surprising, as the local value of SLA/Vcmax in varllvar and LLS is close to the mean CWM values used in fixrecalcllvar. In contrast, Figure 8c shows that using site-specific trait values at Laqueuille (where CWM has higher Vcmax/LLS and lower SLA) reduces the underestimation of GPP by ORCHIDEE compared to the observed GPP, particularly in the summer (i.e., June and August). This trend is also observed in early summer 2023 (i.e., June and July) at Col du Lautaret. However, from July, the simulated GPP in varllvar becomes higher than the observed GPP, with a greater positive error in the varllvar case (Figure 8b). At Col du Lautaret there is a large drop in GPP after July, which is not represented in ORCHIDEE, which maintains a high GPP until September. Since varllvar has a higher GPP than fixrecalcllvar, the positive difference after July is enhanced.

4 | Discussion

A major result is that introducing the spatial variability of traits reduces the NPP spatial variations and gives a better agreement with MODIS NPP. This is due to the decrease in the simulated NPP in the plain and some of the mid-elevation grasslands (with higher SLA and lower Vcmax/LLS), which are the most productive, whereas, on the contrary, an increase on NPP high mountain and Mediterranean grasslands (with lower SLA and higher Vcmax/LLS) which are less productive. The robustness of the results is revealed when assessing the simulated GPP by ORCHIDEE LSM using an independent product based on flux tower observations rather than remote-sensing data (i.e., FLUXCOM GPP). Indeed, the two maps indicate a very similar pattern in regions where incorporating community-level spatial trait variability improves the NPP/GPP simulation relative to the observations (Figure 6a,b). In addition, on-site evaluations support this idea, since using locally adapted trait values (especially at high-elevation grasslands (i.e., Col du Lautaret and Laqueuille) for each local trait has the highest deviation from the standard one) improves GPP simulation during the growing season. This is also in agreement with a study where considering plant functional traits correlations strongly influences the simulated GPP of C3 grasslands by the Australian land surface model (CABLE LSM) (Wang et al. 2023) and reduces the uncertainty associated with model predictions. Furthermore, the results affirmed that GPP and NPP are improved in multiple PFTs, including C3 grasslands, after the inclusion of trait-based data in JULES LSM (Harper et al. 2016, 2018).

Coupling the LLS with SLA and Vcmax enhances the contrast between increased/decreased NPP regions compared to the case where LLS is 64 days, as LLS is, like Vcmax, anti-correlated

13652699, 0, Downloaded from https://onlinelibrary.wiley.com/doi/10.1111/jbi.15079 by MPI 322 Chemical Ecology, Wiley Online Library on [16/01/2025]. See the Terms and Conditions (https://onlinelibrary.wiley.com/terms-and-conditions) on Wiley Online Library for rules of use; OA articles are governed by the applicable Creative Commons License

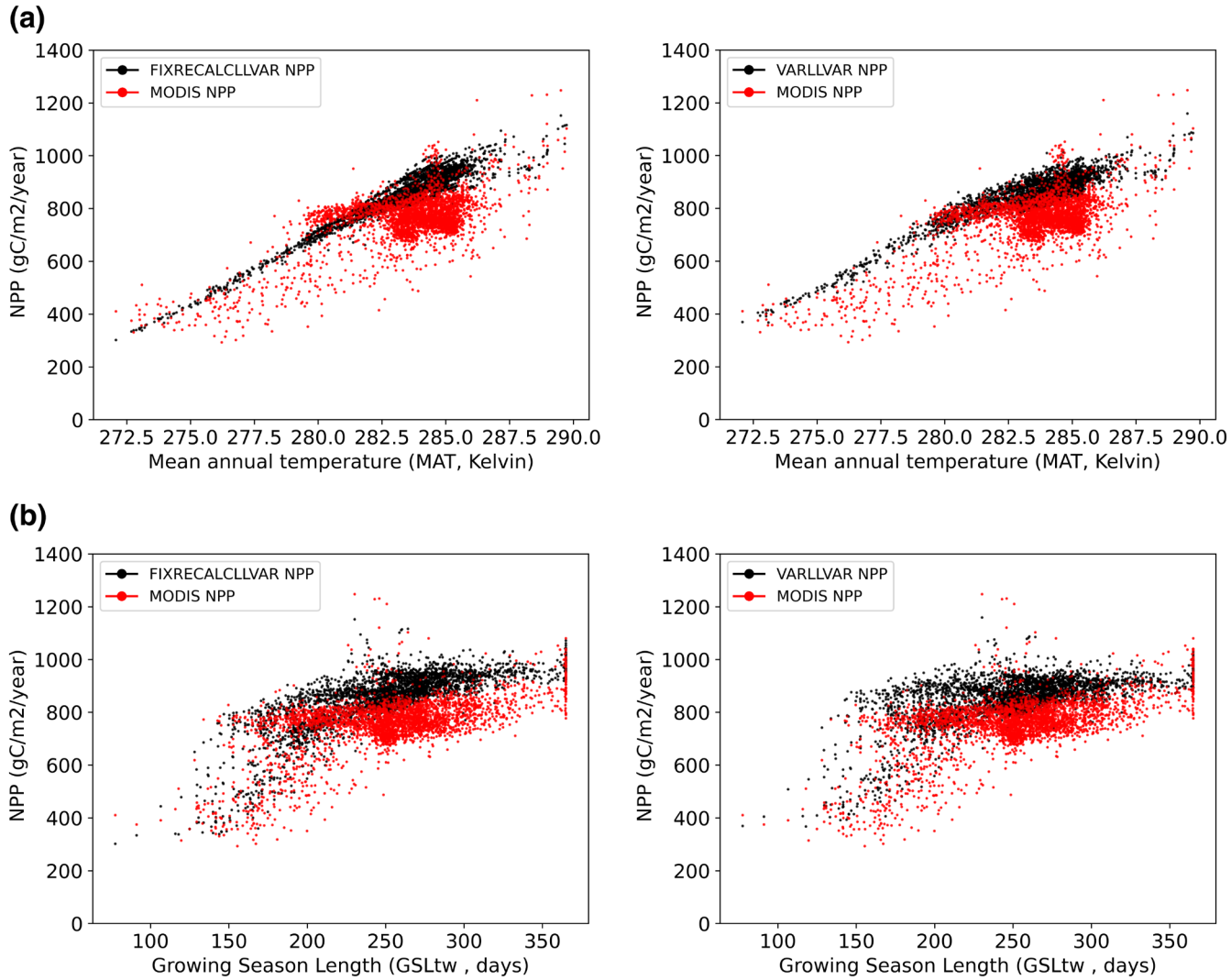

FIGURE 5 | Scatterplots between the mean simulated/estimated NPP for the 2001–2019 time period in function of (a) MAT (Kelvin) and (b) GSL (days).

to SLA. The reduction of the range of NPP in the varllvar simulation is also visible in the relationship between MAT and NPP (Figure 5a). Compared to fixrecalcllvar, varllvar has a higher NPP for the lowest values of MAT and a lower NPP value for higher MAT. We can also see in this figure that, even if the response of NPP to MAT is almost linear for both simulations, there is a small saturation of NPP for higher MAT in varllvar, which is more in agreement with MODIS NPP, for which there is a large saturation of NPP on high MAT. The comparison between MODIS NPP and ORCHIDEE simulation also shows that simulated NPP is highly correlated to MAT, which is not the case for MODIS. This is not surprising since modelling cannot reflect all the local variability that impacts surface reflectance (and then MODIS NPP) that is independent of climate conditions (Wang et al. 2023). Spatially, looking at how the varllvar case better agrees or disagrees with MODIS NPP using the $\delta\epsilon$ metrics (Figure 6) shows that there are regions where variable trait simulation is in better agreement with MODIS but also regions where the agreement is less good. However, it is important to notice that better agreement can be found for both pixels with low SLA/high Vcmax (where the simulated NPP is increased) and for the opposite case where SLA is high and Vcmax is low (where the simulated NPP is decreased), indicating that the reduction of the NPP spatial variations over France considering variable traits is in better agreement with observations. Even if the correlation coefficient is more reduced in variable trait simulation cases, the RMSE is also reduced, indicating a lower dispersion. Examining the average response of $\delta\epsilon$ to climate for both MAT and GSL (Figure 7a,b) shows that simulation with trait variability is improved in regions with low MAT or GSL whereas it is on the opposite slightly degraded in regions with high MAT/GSL. The spatial distribution $\delta\epsilon$ (Figure 6) indicates that for regions with low MAT/GSL (i.e., mountains except for the south of the Alps) (Figure 6 regions b and c), $\delta\epsilon$ is largely negative, whereas for regions with high MAT/GSL (plains), there are well-delimited regions where $\delta\epsilon$ is negative but also positive (e.g., the Cotentin, Figure 6 *region a* or southwest of the Massif Central (Figure 6 region d)). Hence, the fact that we consider the specific traits of mountain grassland (i.e., low SLA, high Vcmax) in varllvar increases the simulated NPP, leading to improved results. On the opposite side, for other types of grasslands (where SLA is increased and Vcmax is decreased), the result largely depends on the region considered, which emphasises that considering only the local

13652699, 0, Downloaded from https://onlinelibrary.wiley.com/doi/10.1111/jbi.15079 by MPI 322 Chemical Ecology, Wiley Online Library on [16/01/2025]. See the Terms and Conditions (https://onlinelibrary.wiley.com/terms-and-conditions) on Wiley Online Library for rules of use; OA articles are governed by the applicable Creative Commons License

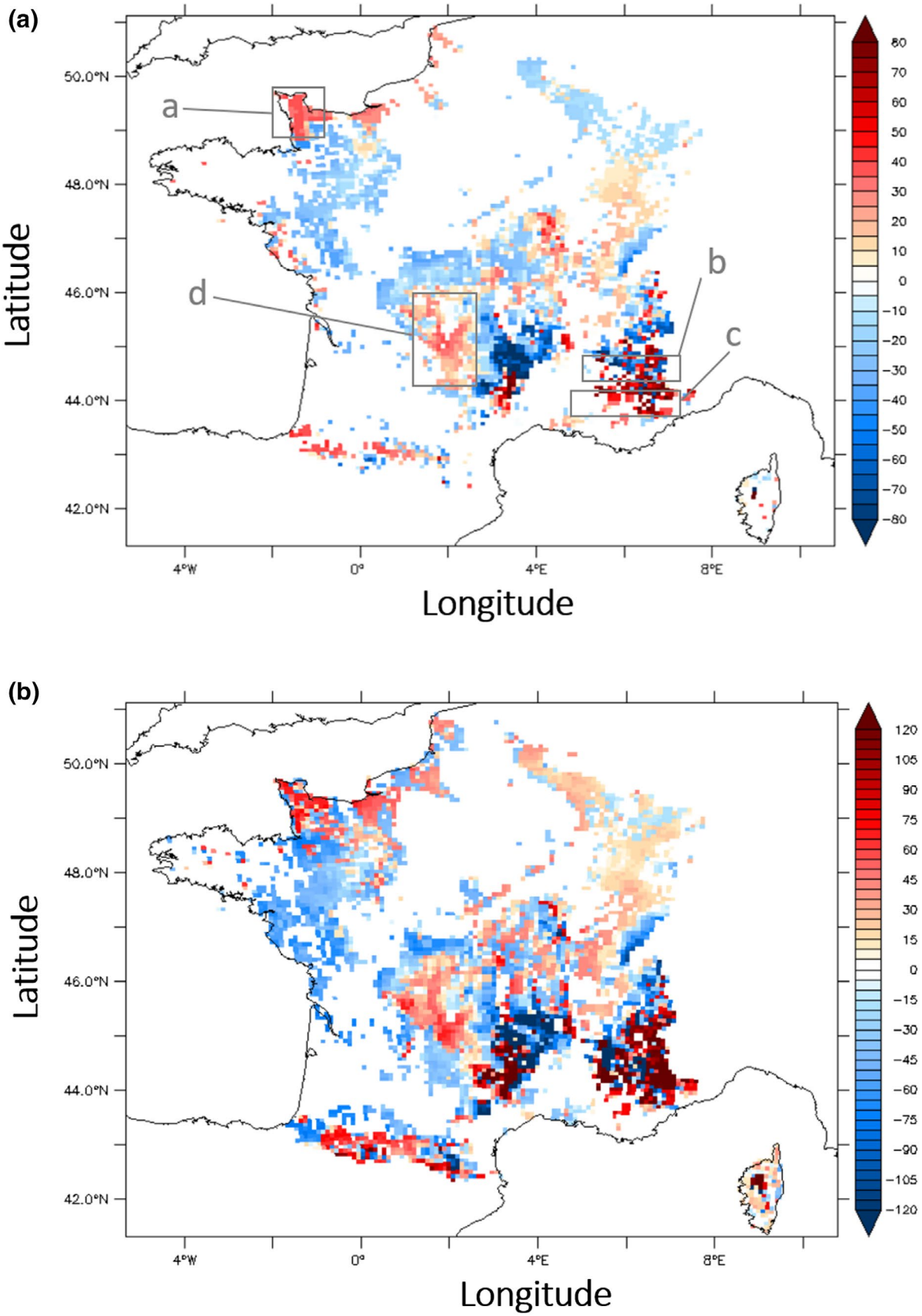

FIGURE 6 | (a) Net primary productivity (NPP) absolute error ($\delta\epsilon$) between varllvar and fixrecalcllvar compared to MODIS NPP for the 2001–2019 time period. Zones a,b,c and d represent the areas cited in Section 3.3. (b) Gross primary productivity (GPP) absolute error ($\delta\epsilon$) between varllvar and fixrecalcllvar compared to FLUXCOM GPP for the 2001–2015 time period.

13652699, 0, Downloaded from https://onlinelibrary.wiley.com/doi/10.1111/jbi.15079 by MPI 322 Chemical Ecology, Wiley Online Library on [16/01/2025]. See the Terms and Conditions (https://onlinelibrary.wiley.com/terms-and-conditions) on Wiley Online Library for rules of use; OA articles are governed by the applicable Creative Commons License

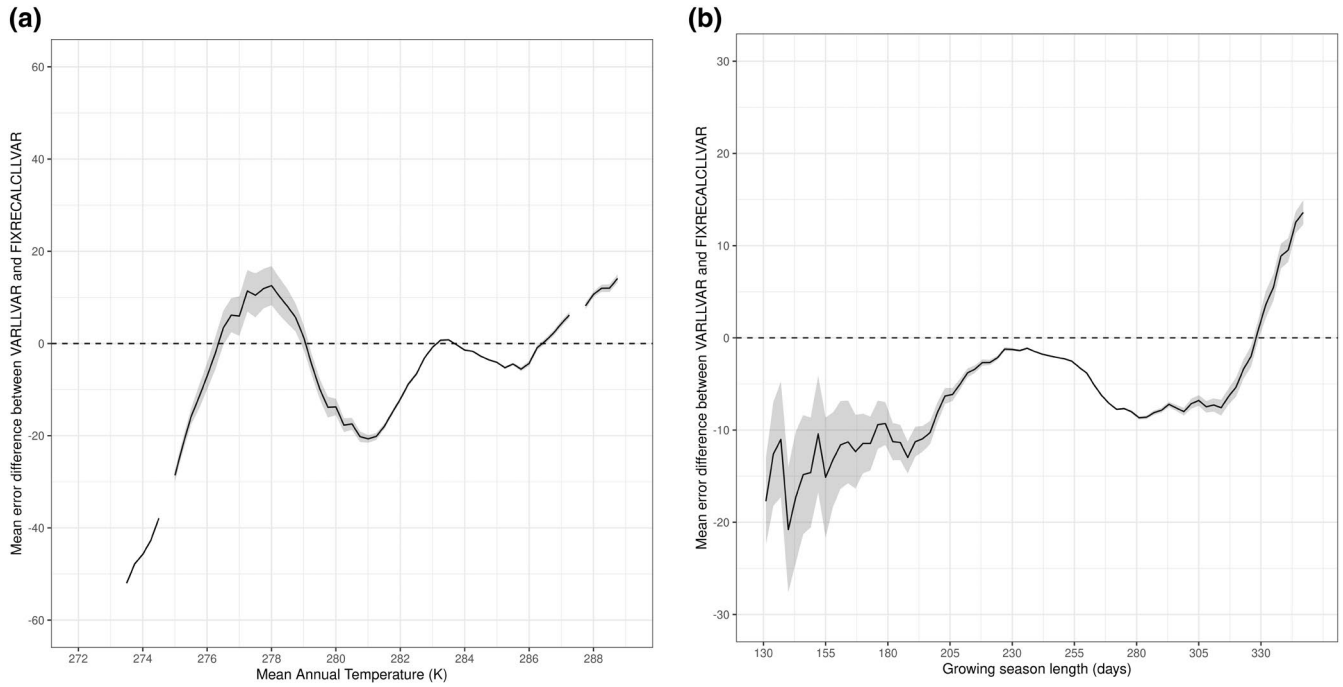

FIGURE 7 | Error difference ($\delta\epsilon$) averaged for each MAT/GSL between varllvar and fixrecalcllvar versus (a) MAT and (b) GSL. The greyed zone represents the variability when permutating data from 10,000 permutations.

characteristics of SLA/Vcmax/LLS is not sufficient to represent the spatial diversity of grassland productivity. It can be related to the fact that we consider only a limited number of traits. This indicates that, in the future, it would be important to also consider other traits. It should also be noted that trait maps were obtained by a non-linear fit of site data using climate (see Section 2.2). It allows covering all the FPGs and is more suitable to use in a modelling approach, but some specific local features and the level of trait variability that is unrelated to climate are not captured by the modelling process of Borgy et al. (2017a). These features could be related to the human-induced nitrogen and phosphorus inputs (Li et al. 2022), plant–soil interactions influenced by biotic and abiotic interactions, and the intraspecific or interspecific trait variations (Zheng et al. 2022), which have a significant impact on the net primary productivity of grasslands.

Looking at the sensitivity of NPP to the observed range of SLA/Vcmax on FPG allows an understanding of how this sensitivity is dependent on climatic conditions. The anticorrelation between SLA and Vcmax values is also reflected in the NPP sensitivity to these parameters. Hence, NPP sensitivity to SLA increases with increasing MAT or GSL but decreases for Vcmax. The sensitivity of NPP to Vcmax is always higher than to SLA. For this reason, coupling SLA with corresponding Vcmax induces a negative sensitivity of NPP to SLA (i.e., NPP decreases with increasing SLA). Except for the response of NPP sensitivity to SLA for MAT (Pearson $R = 0.45$ for decoupled and $R = 0.7$ for coupled), the relationship between the sensitivity of NPP to SLA/Vcmax for MAT or GSL is relatively less pronounced (e.g., $R = 0.2$ for the sensitivity to SLA for GSL).

Considering mean SLA and Vcmax values calculated from trait data increases the productivity of FPGs compared to the SLA and Vcmax values prescribed in the current parameterisation of ORCHIDEE. Prescribing global-scale functional trait values in the ORCHIDEE model does not consistently represent the plant diversity found in the real C3 permanent grasslands (Peaucelle et al. 2019), and seems to be farther from the observations than prescribing fixed or variable trait values from trait data. The variation of plant traits to represent the landscape heterogeneity in LSM and the projections of temporal and spatial dynamics of model parameters (i.e., traits, ecosystem properties) are grand challenges to predict the future of the terrestrial surface and biosphere (Butler et al. 2017; Fisher et al. 2015; Fisher and Koven 2020). The median NPP simulated with the trait data (both with the mean and the variable traits) is higher than the median NPP of the two MODIS products, whereas the original ORCHIDEE simulation is in the lower range of observations. However, the global MODIS NPP is exactly at the mean between the original simulation and the others. Likewise, the difference between the simulations (i.e., fixrecalc, varllfix, fixrecalcllvar, and varllvar) and the global MODIS, is similar to the uncertainty between the two MODIS products. Indeed, even if the two remote sensing products are based on the same MODIS sensor, there is a difference in the median of the two products. A very close pattern is observed when comparing simulated NPP with the two MODIS products after disentangling the two clusters (i.e., 20% of regions with low SLA/high Vcmax and 80% of regions with high SLA/low Vcmax). The Figure S2 shows the spatial difference between those two products. Global MODIS gives a higher NPP compared to European MODIS in most of France except in the Massif Central. Then, there are no regions where both products are fully consistent and demonstrate that MODIS NPP should be considered with caution. While the simulations based on trait data showed a higher NPP compared to both remote sensing estimations, considering the uncertainty in these

13652699, 0, Downloaded from https://onlinelibrary.wiley.com/doi/10.1111/jbi.15079 by MPI 322 Chemical Ecology, Wiley Online Library on [16/01/2025]. See the Terms and Conditions (https://onlinelibrary.wiley.com/terms-and-conditions) on Wiley Online Library for rules of use; OA articles are governed by the applicable Creative Commons License

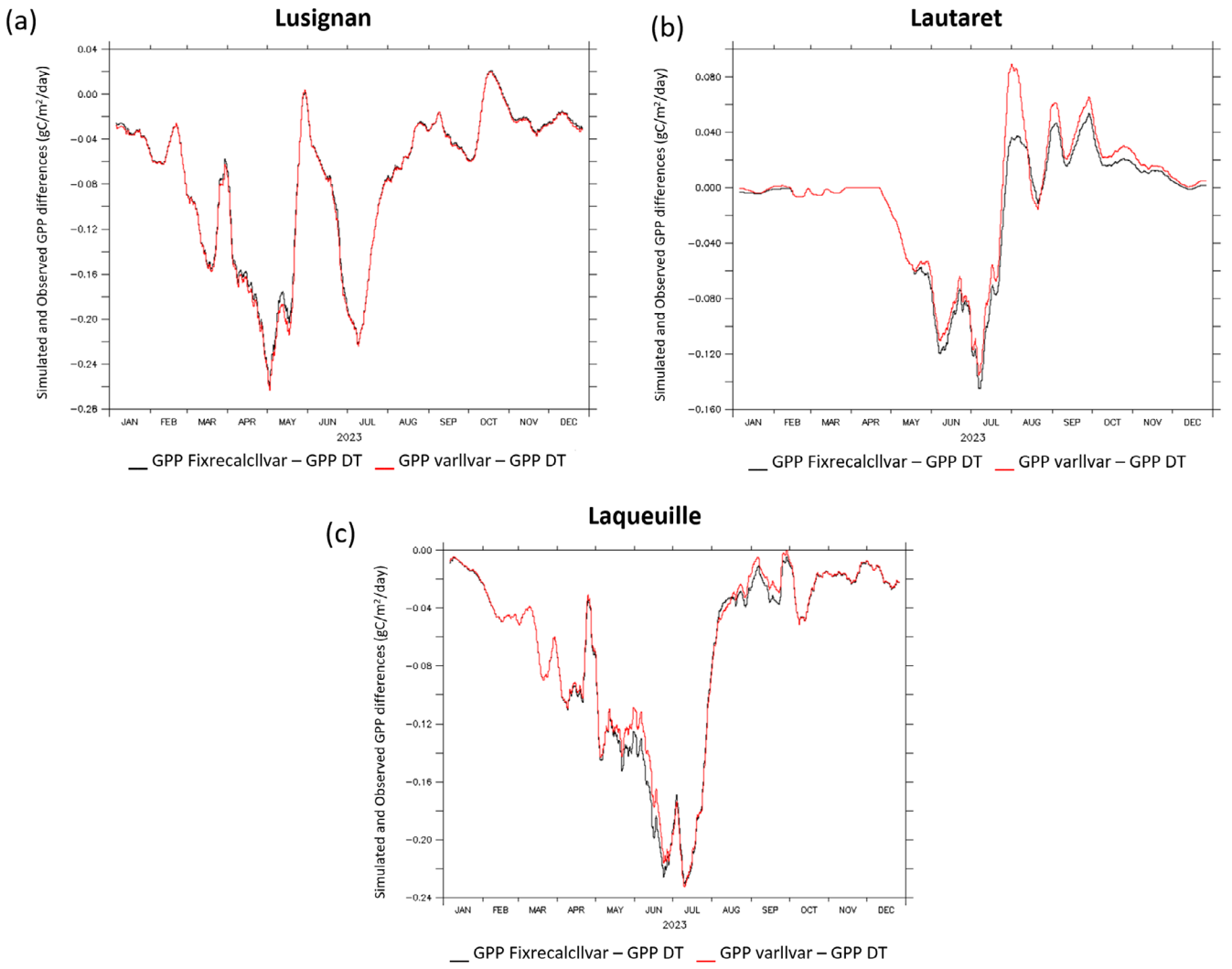

FIGURE 8 | Differences between simulated GPP by ORCHIDEE LSM and observed GPP in daytime (DT) at three sites in France: (a) Lusignan, (b) Col du Lautaret, and (c) Laqueuille.

estimations, the simulated NPP lies within a reasonable range of the MODIS estimation.

It should be noticed that the original low SLA value is associated with greater leaf lifespan (LLS), which is coherent with the observed SLA/LLS from trait data. However, considering the low prescribed SLA value shows a not consistent associated prescribed Vcmax value with the SLA/Vcmax observed relationship based on the trait database (i.e., Vcmax in the model is too low regarding the observed Vcmax). The low SLA and Vcmax explain the low simulated NPP in the standard version compared to simulations with recalculated or variable trait values based on the trait data.

5 | Conclusion and Perspectives

This study showed that the NPP sensitivity to both SLA and Vcmax is partly dependent on climatic conditions. The most constrained climates (particularly mountainous and Mediterranean regions) exhibit a stronger sensitivity to traits. Based on the CWM trait maps, the distribution of traits is highly asymmetrical and essentially separated into two clusters: plains and mountains.

Simulations based on spatially distributed traits, compared to a simulation only based on the mean values of the traits, show higher NPP in mountainous regions with low SLA and high Vcmax and on the contrary, a lower NPP in low-elevation regions with high SLA and low Vcmax. This effect is stronger when we consider the third trait: the leaf life span (LLS), calculated from the leaf economic spectrum. As a result, taking into consideration the spatial traits variation reduces the NPP range over France and creates a more uniform distribution of NPP across France. In other words, local species distribution and abundance play a role in the regulation of the NPP in response to climate. The comparison between the spatial NPP simulated-estimated distribution showed that the reduction of the spatial NPP when varying all traits is more in agreement with remote sensing-based NPP. This is supported by the improvement of the $\delta\varepsilon$ in both regions where NPP is increased or decreased (in variable traits cases compared to spatially fixed traits cases).

13652699, 0, Downloaded from https://onlinelibrary.wiley.com/doi/10.1111/jbi.15079 by MPI 322 Chemical Ecology, Wiley Online Library on [16/01/2025]. See the Terms and Conditions (https://onlinelibrary.wiley.com/terms-and-conditions) on Wiley Online Library for rules of use; OA articles are governed by the applicable Creative Commons License

Considering the relationship between SLA and LLS gives the best agreement. However, the improvement is more evident in cold regions than in cooler ones, where well-defined regions show both improvement and degradation of results compared to MODIS NPP. This can be because only three leaf traits are considered in this study and do not account for all the local conditions such as soil characteristics, land use, etc.

This work underscores the importance of linking functional biogeography and land surface models (LSMs). Despite the unsystematic improvement of productivity in each simulation, considering the spatial variability of SLA, Vcmax, and LLS shows a better compromise, regardless of the coherence between trait values and the proximity to the satellite observations with a better representation of NPP.

In this paper, we have shown that the introduction of CWM trait maps is an effective and doable approach to represent more realistically the plant diversity in FPGs in an LSM such as ORCHIDEE. To integrate other CWM trait maps in ORCHIDEE, providing continuous maps of other functional traits in France, Europe, or the global scale is needed to study the primary productivity variation by accounting for other traits of the leaf economic spectrum. Therefore, due to the complexity of the functional biogeography framework, going towards a trait-flexible model based on the existing databases leads to a better representation of trait trade-offs and plasticity. We acknowledge that the present approach is limited by the lack of trait measurements. For instance, Vcmax and LLS were estimated through relationships with other traits rather than being measured directly. Likewise, only three foliar traits were considered, whereas other important traits are needed to improve the simulation of NPP. This probably explains the fact that accounting for trait variability improves simulations only in certain parts of France. Another limitation is the use of fixed CWM, which does not allow the consideration of the local variation of traits for a given species (i.e., intraspecific trait variability). In the future, in the ecological and modelling field, emphasising the study of both productivity and its temporal stability will be essential for a more resilient ecosystem and more sustainable and effective land management. This emphasises the need to increase the in situ measurements both in space and in time.

Author Contributions

Sara Chebbo led the study design, performed all experiments, analyzed the data, conducted the statistical analysis, interpreted the results, drafted and revised the manuscript under the supervision of Nicolas Viovy. Cyrille Violle and Lucie Mahaut provided the trait data. All co-authors reviewed and approved the final manuscript version and made equal contributions.

Acknowledgements

This work was performed using HPC resources from GENCI-TGCC (Grant 2023-06328) and supported by the CLAND Convergence Institute (France) funded by the French National Research Agency (ANR). No relevant fieldwork permissions were required.

Conflicts of Interest

The authors declare no conflicts of interest.

Data Availability Statement

Codes and scripts are publicly available on https://github.com/nviovy/ORCHIDEE_DIVGRASS.

References

Berzaghi, F., I. J. Wright, K. Kramer, et al. 2020. "Towards a New Generation of Trait-Flexible Vegetation Models." *Trends in Ecology & Evolution* 35, no. 3: 191–205. https://doi.org/10.1016/j.tree.2019.11.006.

Bonan, G. B. 2008. "Forests and Climate Change: Forcings, Feedbacks, and the Climate Benefits of Forests." *Science* 320, no. 5882: 1444–1449. https://doi.org/10.1126/science.1155121.

Borgy, B., C. Violle, P. Choler, et al. 2017a. "Plant Community Structure and Nitrogen Inputs Modulate the Climate Signal on Leaf Traits." *Global Ecology and Biogeography* 26, no. 10: 1138–1152. https://doi.org/10.1111/geb.12623.

Borgy, B., C. Violle, P. Choler, et al. 2017b. "Sensitivity of Community-Level Trait–Environment Relationships to Data Representativeness: A Test for Functional Biogeography." *Global Ecology and Biogeography* 26, no. 6: 729–739. https://doi.org/10.1111/geb.12573.

Butler, E. E., A. Datta, H. Flores-Moreno, et al. 2017. "Mapping Local and Global Variability in Plant Trait Distributions." *Proceedings of the National Academy of Sciences of the United States of America* 114, no. 51: E10937–E10946. https://doi.org/10.1073/pnas.1708984114.

Chacón-Labella, J., C. Hinojo-Hinojo, T. Bohner, et al. 2023. "How to Improve Scaling from Traits to Ecosystem Processes." *Trends in Ecology & Evolution* 38, no. 3: 228–237. https://doi.org/10.1016/j.tree.2022.10.007.

Cramer, W., A. Bondeau, F. I. Woodward, et al. 2001. "Global Response of Terrestrial Ecosystem Structure and Function to CO_2 and Climate Change: Results From Six Dynamic Global Vegetation Models." *Global Change Biology* 7, no. 4: 357–373. https://doi.org/10.1046/j.1365-2486.2001.00383.x.

de Bello, F., S. Lavorel, S. Díaz, et al. 2010. "Towards an assessment of multiple ecosystem processes and services via functional traits." *Biodiversity and Conservation* 19: 2873–2893.

Denelle, P., C. Violle, and F. Munoz. 2020. "Generalist Plants Are More Competitive and More Functionally Similar to Each Other Than Specialist Plants: Insights From Network Analyses." *Journal of Biogeography* 47, no. 9: 1922–1933. https://doi.org/10.1111/jbi.13848.

Dias, A. T. C., M. P. Berg, F. de Bello, A. R. Van Oosten, K. Bílá, and M. Moretti. 2013. "An Experimental Framework to Identify Community Functional Components Driving Ecosystem Processes and Services Delivery." *Journal of Ecology* 101, no. 1: 29–37. https://doi.org/10.1111/1365-2745.12024.

Díaz, S., J. Kattge, J. H. C. Cornelissen, et al. 2016. "The Global Spectrum of Plant Form and Function." *Nature* 529, no. 7585: 167–171. https://doi.org/10.1038/nature16489.

Díaz, S., S. Lavorel, F. S. Chapin, P. A. Tecco, D. E. Gurvich, and K. Grigulis. 2007. "Functional Diversity — at the Crossroads Between Ecosystem Functioning and Environmental Filters." https://doi.org/10.1007/978-3-540-32730-1_7.

Ducoudré, N., K. Laval, and A. Perrier. 1992. "SECHIBA, a New Set of Parameterizations of the Hydrologic Exchanges at the Land-Atmosphere Interface Within the LMD Atmospheric General Circulation Model." *Journal of Climate* 6, no. 2: 248–273.

Enquist, B. J., J. Norberg, S. P. Bonser, et al. 2015. "Scaling From Traits to Ecosystems: Developing a General Trait Driver Theory via Integrating Trait-Based and Metabolic Scaling Theories." *In Advances in Ecological Research* 52: 249–318. https://doi.org/10.1016/bs.aecr.2015.02.001.

Fisher, R. A., and C. D. Koven. 2020. "Perspectives on the Future of Land Surface Models and the Challenges of Representing Complex

13652699, 0, Downloaded from https://onlinelibrary.wiley.com/doi/10.1111/jbi.15079 by MPI 322 Chemical Ecology, Wiley Online Library on [16/01/2025]. See the Terms and Conditions (https://onlinelibrary.wiley.com/terms-and-conditions) on Wiley Online Library for rules of use; OA articles are governed by the applicable Creative Commons License

Terrestrial Systems." *Journal of Advances in Modeling Earth Systems* 12, no. 4: e2018MS001453. https://doi.org/10.1029/2018MS001453.

Fisher, R. A., C. D. Koven, W. R. L. Anderegg, et al. 2018. "Vegetation Demographics in Earth System Models: A Review of Progress and Priorities." *Global Change Biology* 24, no. 1: 35–54. https://doi.org/10.1111/gcb.13910.

Fisher, R. A., S. Muszala, M. Verteinstein, et al. 2015. "Taking off the Training Wheels: The Properties of a Dynamic Vegetation Model Without Climate Envelopes, CLM4.5(ED)." *Geoscientific Model Development* 8: 3593–3619.

Foley, J. A., I. C. Prentice, N. Ramankutty, et al. 1996. "An Integrated Biosphere Model of Land Surface Processes, Terrestrial Carbon Balance, and Vegetation Dynamics." *Global Biogeochemical Cycles* 10, no. 4: 603–628. https://doi.org/10.1029/96GB02692.

Friedlingstein, P., M. W. Jones, M. O'Sullivan, et al. 2022. "Global Carbon Budget 2021." *Earth System Science Data* 14, no. 4: 1917–2005. https://doi.org/10.5194/essd-14-1917-2022.

Garnier, E., J. Cortez, G. Billès, et al. 2004. "Plant Functional Markers Capture Ecosystem Properties During Secondary Succession." *Ecology* 85, no. 9: 2630–2637. https://doi.org/10.1890/03-0799.

Garnier, E., M.-L. Navas, and K. Grigulis. 2015. *Plant Functional Diversity: Organism Traits, Community Structure, and Ecosystem Properties*. Oxford University Press. https://doi.org/10.1093/acprof:oso/9780198757368.001.0001.

Gijbels, I., and I. Prosdocimi. 2010. "Loess." *Wiley Interdisciplinary Reviews: Computational Statistics* 2, no. 5: 590–599. https://doi.org/10.1002/wics.104.

Harper, A. B., P. M. Cox, P. Friedlingstein, et al. 2016. "Improved Representation of Plant Functional Types and Physiology in the Joint UK Land Environment Simulator (JULES v4.2) Using Plant Trait Information." *Geoscientific Model Development* 9, no. 7: 2415–2440. https://doi.org/10.5194/gmd-9-2415-2016.

Harper, A. B., A. J. Wiltshire, P. M. Cox, et al. 2018. "Vegetation Distribution and Terrestrial Carbon Cycle in a Carbon Cycle Configuration of JULES4.6 With New Plant Functional Types." *Geoscientific Model Development* 11, no. 7: 2857–2873. https://doi.org/10.5194/gmd-11-2857-2018.

Jung, M., C. Schwalm, M. Migliavacca, et al. 2020. "Scaling Carbon Fluxes From Eddy Covariance Sites to Globe: Synthesis and Evaluation of the FLUXCOM Approach." *Biogeosciences* 17, no. 5: 1343–1365. https://doi.org/10.5194/bg-17-1343-2020.

Kattge, J., G. Bönisch, S. Díaz, et al. 2020. "TRY Plant Trait Database – Enhanced Coverage and Open Access." *Global Change Biology* 26, no. 1: 119–188. https://doi.org/10.1111/gcb.14904.

Kattge, J., S. Díaz, S. Lavorel, et al. 2011. "TRY – a Global Database of Plant Traits." *Global Change Biology* 17, no. 9: 2905–2935. https://doi.org/10.1111/j.1365-2486.2011.02451.x.

Kattge, J., W. Knorr, T. Raddatz, and C. Wirth. 2009. "Quantifying Photosynthetic Capacity and Its Relationship to Leaf Nitrogen Content for Global-Scale Terrestrial Biosphere Models." *Global Change Biology* 15, no. 4: 976–991. https://doi.org/10.1111/j.1365-2486.2008.01744.x.

Krinner, G., N. Viovy, N. de Noblet-Ducoudré, et al. 2005. "A Dynamic Global Vegetation Model for Studies of the Coupled Atmosphere-Biosphere System." *Global Biogeochemical Cycles* 19, no. 1: 1–33. https://doi.org/10.1029/2003GB002199.

Lavorel, S., and E. Garnier. 2002. "Predicting Changes in Community Composition and Ecosystem Functioning From Plant Traits: Revisiting the Holy Grail." *Functional Ecology* 16, no. 5: 545–556. https://doi.org/10.1046/j.1365-2435.2002.00664.x.

Lavorel, S., and K. Grigulis. 2012. "How Fundamental Plant Functional Trait Relationships Scale-Up to Trade-Offs and Synergies in Ecosystem Services." *Journal of Ecology* 100, no. 1: 128–140. https://doi.org/10.1111/j.1365-2745.2011.01914.x.

Lavorel, S., S. McIntyre, J. Landsberg, and T. D. A. Forbes. 1997. "Plant Functional Classifications: From General Groups to Specific Groups Based on Response to Disturbance." *Trends in Ecology & Evolution* 12, no. 12: 474–478. https://doi.org/10.1016/S0169-5347(97)01219-6.

Lepš, J., F. de Bello, P. Šmilauer, and J. Doležal. 2011. "Community Trait Response to Environment: Disentangling Species Turnover vs Intraspecific Trait Variability Effects." *Ecography* 34, no. 5: 856–863. https://doi.org/10.1111/j.1600-0587.2010.06904.x.

Li, W., X. Gan, Y. Jiang, et al. 2022. "Nitrogen Effects on Grassland Biomass Production and Biodiversity Are Stronger Than Those of Phosphorus." *Environmental Pollution* 309: 119720. https://doi.org/10.1016/j.envpol.2022.119720.

Messina, P., J. Lathière, K. Sindelarova, et al. 2016. "Global Biogenic Volatile Organic Compound Emissions in the ORCHIDEE and MEGAN Models and Sensitivity to Key Parameters." *Atmospheric Chemistry and Physics* 16, no. 22: 14169–14202. https://doi.org/10.5194/acp-16-14169-2016.

Moulin, S., L. Kergoat, N. Viovy, and G. Dedieu. 1997. "Global-Scale Assessment of Vegetation Phenology Using NOAA/AVHRR Satellite Measurements." *Journal of Climate* 10, no. 6: 1154–1170. https://doi.org/10.1175/1520-0442(1997)010<1154:GSAOVP>2.0.CO;2.

Neumann, M., A. Moreno, C. Thurnher, et al. 2016. "Creating a Regional MODIS Satellite-Driven Net Primary Production Dataset for European Forests." *Remote Sensing* 8, no. 7: 554. https://doi.org/10.3390/rs8070554.

Pan, Q., H. Zheng, Z. H. Wang, Z. Wen, and Y. Yan-Zheng. 2021. "Effects of Plat Functional Traits on Ecosystem Services: A Review. In Chinese." *Journal of Plant Ecology* 45, no. 6: 1140–1153.

Pavlick, R., D. T. Drewry, K. Bohn, B. Reu, and A. Kleidon. 2013. "The Jena Diversity-Dynamic Global Vegetation Model (JeDi-DGVM): A Diverse Approach to Representing Terrestrial Biogeography and Biogeochemistry Based on Plant Functional Trade-Offs." *Biogeosciences* 10, no. 6: 4137–4177. https://doi.org/10.5194/bg-10-4137-2013.

Peaucelle, M., C. Bacour, P. Ciais, et al. 2019. "Covariations Between Plant Functional Traits Emerge From Constraining Parameterization of a Terrestrial Biosphere Model." *Global Ecology and Biogeography* 28, no. 9: 1351–1365. https://doi.org/10.1111/geb.12937.

Peaucelle, M., V. Bellassen, P. Ciais, J. Peñuelas, and N. Viovy. 2017. "A New Approach to Optimal Discretization of Plant Functional Types in a Process-Based Ecosystem Model With Forest Management: A Case Study for Temperate Conifers." *Global Ecology and Biogeography* 26, no. 4: 486–499. https://doi.org/10.1111/geb.12557.

Penone, C., A. D. Davidson, K. T. Shoemaker, et al. 2014. "Imputation of Missing Data in Life-History Trait Datasets: Which Approach Performs the Best?" *Methods in Ecology and Evolution* 5, no. 9: 961–970. https://doi.org/10.1111/2041-210X.12232.

Plantureux, S., E. Pottier, and P. Carrère. 2012. "La prairie permanente: nouveaux enjeux, nouvelles définitions?" *Fourrages* 211: 181–193.

Reich, P. B., D. S. Ellsworth, M. B. Walters, et al. 1999. "Generality of Leaf Trait Relationships: A Test Across Six Biomes." *Ecology* 80, no. 6: 1955–1969.

Reichstein, M., M. Bahn, M. D. Mahecha, J. Kattge, and D. D. Baldocchi. 2014. "Linking Plant and Ecosystem Functional Biogeography." *Proceedings of the National Academy of Sciences of the United States of America* 111, no. 38: 13697–13702. https://doi.org/10.1073/pnas.1216065111.

Running, S. W., R. Nemani, J. M. Glassy, and P.E. Thornton. 1999. "MODIS DAILY PHOTOSYNTHESIS (PSN) AND ANNUAL NET PRIMARY PRODUCTION (NPP) PRODUCT (MOD17) Algorithm Theoretical Basis Document." https://www.umt.edu/numerical-terradynamic-simulation-group/files/modis/atbd_mod17_v21.pdf.

13652699, 0, Downloaded from https://onlinelibrary.wiley.com/doi/10.1111/jbi.15079 by MPI 322 Chemical Ecology, Wiley Online Library on [16/01/2025]. See the Terms and Conditions (https://onlinelibrary.wiley.com/terms-and-conditions) on Wiley Online Library for rules of use; OA articles are governed by the applicable Creative Commons License

Sabbatini, S., I. Mammarella, N. Arriga, et al. 2018. "Eddy Covariance Raw Data Processing for CO_2 and Energy Fluxes Calculation at ICOS Ecosystem Stations." *International Agrophysics* 32, no. 4: 495–515.

Sakschewski, B., W. von Bloh, A. Boit, et al. 2015. "Leaf and Stem Economics Spectra Drive Diversity of Functional Plant Traits in a Dynamic Global Vegetation Model." *Global Change Biology* 21, no. 7: 2711–2725. https://doi.org/10.1111/gcb.12870.

Shipley, B., D. Vile, and É. Garnier. 2006. "From Plant Traits to Plant Communities: A Statistical Mechanistic Approach to Biodiversity." *Science* 314, no. 5800: 812–814. https://doi.org/10.1126/science.1131344.

Sitch, S., B. Smith, I. C. Prentice, et al. 2003. "Evaluation of Ecosystem Dynamics, Plant Geography and Terrestrial Carbon Cycling in the LPJ Dynamic Global Vegetation Model." *Global Change Biology* 9, no. 2: 161–185. https://doi.org/10.1046/j.1365-2486.2003.00569.x.

Van Bodegom, P. M., J. C. Douma, and L. M. Verheijen. 2014. "A Fully Traits-Based Approach to Modeling Global Vegetation Distribution." *Proceedings of the National Academy of Sciences of the United States of America* 111, no. 38: 13733–13738. https://doi.org/10.1073/pnas.1304551110.

Van Bodegom, P. M., J. C. Douma, J. P. M. Witte, J. C. Ordoñez, R. P. Bartholomeus, and R. Aerts. 2012. "Going Beyond Limitations of Plant Functional Types When Predicting Global Ecosystem-Atmosphere Fluxes: Exploring the Merits of Traits-Based Approaches." *Global Ecology and Biogeography* 21, no. 6: 625–636. https://doi.org/10.1111/j.1466-8238.2011.00717.x.

Verheijen, L. M., R. Aerts, V. Brovkin, et al. 2015. "Inclusion of Ecologically Based Trait Variation in Plant Functional Types Reduces the Projected Land Carbon Sink in an Earth System Model." *Global Change Biology* 21, no. 8: 3074–3086. https://doi.org/10.1111/gcb.12871.

Vidal, J. P., E. Martin, L. Franchistéguy, M. Baillon, and J. M. Soubeyroux. 2010. "A 50-Year High-Resolution Atmospheric Reanalysis Over France With the Safran System." *International Journal of Climatology* 30, no. 11: 1627–1644. https://doi.org/10.1002/joc.2003.

Violle, C., P. Choler, B. Borgy, et al. 2015. "Vegetation Ecology Meets Ecosystem Science: Permanent Grasslands as a Functional Biogeography Case Study." *Science of the Total Environment* 534: 43–51. https://doi.org/10.1016/j.scitotenv.2015.03.141.

Violle, C., M. L. Navas, D. Vile, et al. 2007. "Let the concept of trait be functional!" *Oikos* 116, no. 5: 882–892. https://doi.org/10.1111/j.0030-1299.2007.15559.x.

Violle, C., P. B. Reich, S. W. Pacala, B. J. Enquist, and J. Kattge. 2014. "The Emergence and Promise of Functional Biogeography." *Proceedings of the National Academy of Sciences of the United States of America* 111, no. 38: 13690–13696.

Viovy, N., and N. de Noblet. 1997. "Coupling Water and Carbon Cycle in the Biosphere./Couplage du cycle de l'eau et du Carbone dans la Biosphère." *Sciences Géologiques. Bulletin* 50, no. 1: 109–121. https://doi.org/10.3406/sgeol.1997.1948.

Wang, Y., R. K. Braghiere, M. Longo, et al. 2023. "Modeling Global Vegetation Gross Primary Productivity, Transpiration and Hyperspectral Canopy Radiative Transfer Simultaneously Using a Next Generation Land Surface Model—CliMA Land." *Journal of Advances in Modeling Earth Systems* 15: e2021MS002964. https://doi.org/10.1029/2021MS002964.

Wright, I. J., P. B. Reich, M. Westoby, et al. 2004. "The Worldwide Leaf Economics Spectrum." *Nature* 428, no. 6985: 821–827. https://doi.org/10.1038/nature02403.

Zheng, S., Y. Chi, X. Yang, W. Li, Z. Lan, and Y. Bai. 2022. "Direct and Indirect Effects of Nitrogen Enrichment and Grazing on Grassland Productivity Through Intraspecific Trait Variability." *Journal of Applied Ecology* 59, no. 2: 598–610. https://doi.org/10.1111/1365-2664.14078.

Supporting Information

Additional supporting information can be found online in the Supporting Information section.

13652699, 0, Downloaded from https://onlinelibrary.wiley.com/doi/10.1111/jbi.15079 by MPI 322 Chemical Ecology, Wiley Online Library on [16/01/2025]. See the Terms and Conditions (https://onlinelibrary.wiley.com/terms-and-conditions) on Wiley Online Library for rules of use; OA articles are governed by the applicable Creative Commons License